Magnetotransport patterns of collective localization near $\nu = 1$ in a high-mobility two-dimensional electron gas

S. A. Myers,[1] Haoyun Huang,[1] L. N. Pfeiffer,[2] K. W. West,[2] and G. A. Csáthy[1]
[1]*Department of Physics and Astronomy, Purdue University, West Lafayette, Indiana 47907, USA*
[2]*Department of Electrical Engineering, Princeton University, Princeton, New Jersey 08544, USA*

(Received 30 April 2021; revised 12 July 2021; accepted 13 July 2021; published 21 July 2021)

We report complex magnetotransport patterns of the $\nu = 1$ integer quantum Hall state in a GaAs/AlGaAs sample from the newest generation with a record high electron mobility. The reentrant integer quantum Hall effect in the flanks of the $\nu = 1$ plateau indicates the formation of the integer quantum Hall Wigner solid, a collective insulator. Moreover, at a fixed filling factor, the longitudinal resistance versus temperature in the region of the integer quantum Hall Wigner solid exhibits a sharp peak. Such sharp peaks in the longitudinal resistance versus temperature so far were only detected for bubble phases forming in high Landau levels but were absent in the region of the Anderson insulator. We suggest that in samples of sufficiently low disorder, sharp peaks in the longitudinal resistance versus temperature traces are universal transport signatures of all isotropic electron solids that form in the flanks of integer quantum Hall plateaus. We discuss possible origins of these sharp resistance peaks and we draw a stability diagram for the insulating phases in the ν-T phase space.

DOI: 10.1103/PhysRevB.104.045311

I. INTRODUCTION: SINGLE ELECTRON AND COLLECTIVE LOCALIZATION ON AN INTEGER QUANTUM HALL PLATEAU

Electron localization plays an important role in topological materials. This is because transport supported by the boundary states of these materials is protected when electrons in the bulk are localized. These ideas [1–3] were introduced in order to explain the plateaus of integer quantum Hall states (IQHS) that form in the two-dimensional electron gas (2DEG) [4], and then later extended to other topological materials.

Over the years, the concept of electron localization has evolved. It was realized that in order to understand localization along a plateau of an IQHS, both single particle and collective localization had to be invoked. According to current understanding, an Anderson insulator (AI) forms near the center of an integer quantum Hall plateau at low quasiparticle densities. However, as the quasiparticle density is increased past the range of the AI, electrons in 2DEGs of sufficiently low disorder reorganize themselves in collective insulators called charge density waves [5–9]. These charge density waves are pinned by the disorder, hence their insulating behavior. One example of such a collective insulator is the Wigner solid forming in the flanks of an integer quantum Hall plateau, also referred to as the integer quantum Hall Wigner solid (IQHWS) [10–12]; the IQHWS is related to the Wigner solid forming at the largest magnetic fields [13–15]. In high Landau levels, a further increase of the quasiparticle density leads to the formation of the electronic bubble phases (BPs) and of stripe phases [5–9,16–21]. These collective insulators were discovered in 2DEGs confined to GaAs/AlGaAs interfaces [10–21], but recently BPs [22] and IQHWSs [23] were also observed in high-quality graphene.

The isotropic insulating phases near an integer plateau, i.e., the AI, IQHWS, and BPs, all exhibit the same transport behavior: they have a vanishing magnetoresistance $R_{xx} = 0$ and a Hall resistance quantized to the value of a nearby integer plateau, $R_{xy} = h/ie^2$, where i is an integer. Nonetheless, BPs are separated from other localized states that form in the middle of an integer plateau by a conspicuous deviation of magnetotransport from quantization. Such a behavior is commonly referred to as reentrance of the integer quantum Hall effect [17,18]. In contrast, a similar reentrant transport is typically absent between the IQHWS and the AI. Therefore, in order to distinguish the IQHWS from the AI, techniques other than transport were developed. Examples of such techniques are absorption in the microwave frequency domain [10–12], compressibility [24], nuclear magnetic resonance [25], surface acoustic wave propagation [26], and tunneling measurements [27]. The continued absence of any features in magnetoresistance separating the IQHWS and the AI brought into question whether or not dc transport could successfully differentiate the IQHWS from the AI.

Transport features separating the IQHWS from the middle part of the integer quantum Hall plateau akin to reentrance of the integer quantum Hall effect were reported in low-disorder GaAs samples [28] and, more recently, in graphene [23]. However, there is limited data available in this region. Here we present a collection of stunning magnetotransport patterns from the newest generation of ultralow-disorder GaAs samples [29]. Reentrant transport in the flanks of the $\nu = 1$ IQHS is associated with the IQHWS. We further investigate the IQHWS by analyzing the longitudinal resistance versus temperature traces at fixed filling factors, or $R_{xx}(T)|_{\nu=\text{fixed}}$. We find that $R_{xx}(T)|_{\nu=\text{fixed}}$ traces exhibit a sharp peak in the IQHWS region, but such sharp peaks are absent for the AI.

The temperature of this sharp peak is interpreted as the onset of the IQHWS. In higher Landau levels, sharp peaks that resemble those reported in the present work have been observed for all multielectron BPs [30–33]. We thus surmise that sharp peaks in $R_{xx}(T)|_{\nu=\text{fixed}}$ are likely a universal property of the isotropic electron solids. In the following, we discuss possible origins of such sharp resistance peaks and we draw a stability diagram for the AI and the IQHWS forming near $\nu = 1$ in the ν-T phase space.

II. SAMPLE DETAILS AND EXPERIMENTAL TECHNIQUES

Recent efforts of source-material purification and innovation in the GaAs molecular beam epitaxy technique produced 2DEGs with record high mobilities [29]. Our measurements were performed on a sample that belongs to this newest generation, with an electron density $n = 7.5 \times 10^{10}$ cm^{-2} and a low-temperature mobility of $\mu = 24 \times 10^6$ cm^2/V s. At this electron density, the mobility exceeds that of samples from an earlier generation by more than a factor of two [29]. The width of the confining quantum well is 58.5 nm. Our sample was cleaved to 4×4 mm^2 size with eight indium contacts in the van der Pauw geometry, and it was mounted in a He-3 immersion cell [34] in order to stabilize the electron temperature. The sample state was prepared by a brief illumination with a red light emitting diode. Simultaneous longitudinal resistance R_{xx} and Hall resistance R_{xy} measurements were performed using two lock-in amplifiers with a current excitation of 3 nA and a frequency of 13.3 Hz.

III. MAGNETOTRANSPORT NEAR THE $\nu = 1$ INTEGER QUANTUM HALL PLATEAU

The longitudinal magnetoresistance R_{xx} and the Hall resistance R_{xy} are measured at several temperatures. Representative traces are shown in Fig. 1. In this figure, we marked the IQHSs at $\nu = 1$ and 2 as well as the fractional quantum Hall states observed at $\nu = 5/3, 4/3$, and $4/5$. At $T = 95$ mK, the measured magnetoresistance $R_{xx}(B)|_{T=\text{fixed}}$ close to $\nu = 1$ is typical for that of an integer quantum Hall state: R_{xx} vanishes over a range of magnetic fields of about 0.2 T and $R_{xy} = h/e^2$ in the same range of fields. However, as the temperature is lowered, a more complex structure develops. For example, at $T = 55$ mK, there is a local minimum developing in R_{xx} near $B = 3.5$ T. This local minimum is marked by an arrow in Fig. 1 and it is located between two local maxima marked by the $*$ symbols. A further lowering of the temperature to $T = 45$ mK results in a deeper resistance minimum in R_{xx} and in a fully quantized R_{xy} near $B = 3.5$ T. The sequence of vanishing R_{xx} in the center of the integer plateau, a local maximum in R_{xx} near $B = 3.3$ T, and the vanishing R_{xx} near $B = 3.5$ T signals a reentrance of the integer quantum Hall plateau. Following arguments put forth earlier [17,18,28], such a reentrant behavior is not expected for the AI and hence the region of the local minimum in R_{xx} near $B = 3.5$ T is associated with a collective insulator. We observe a similar collective insulator on the other flank of the $\nu = 1$ integer quantum Hall plateau near $B = 2.75$ T.

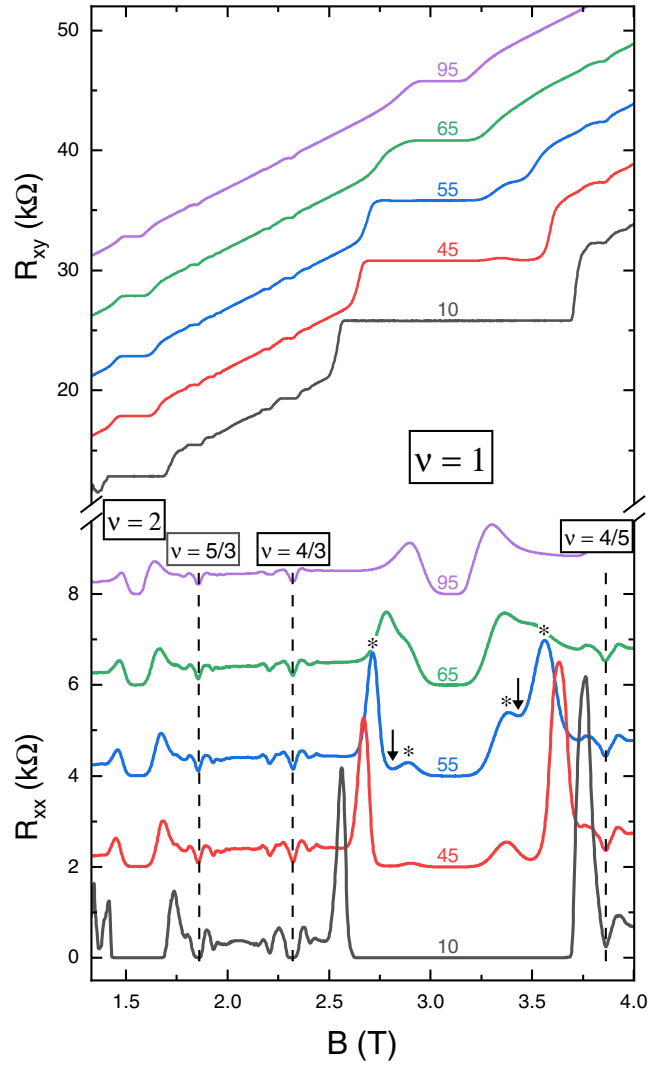

FIG. 1. The evolution of the longitudinal magnetoresistance R_{xx} and Hall resistance R_{xy} plotted against the magnetic field B at several temperatures. Labels in boxes mark integer and fractional quantum Hall states, whereas numbers indicate temperatures in mK. R_{xx} traces other than the one at $T = 10$ mK are offset by 2 kΩ. Similarly, R_{xy} traces other than the one at $T = 10$ mK are offset by 5 kΩ. For the R_{xx} trace at $T = 55$ mK, arrows mark reentrant integer quantum Hall states associated with the IQHWS, while the $*$ symbols mark consecutive local maxima in R_{xx} between which the IQHWSs form.

For insight on the nature of the collective insulators in the flanks of the $\nu = 1$ IQHS, we examine the Landau level filling factors at which they develop. In Fig. 2, we show a series of R_{xx} traces against ν over an extended range of temperatures. The collective insulators near $B = 2.75$ T and $B = 3.5$ T are seen in Fig. 2 near the filling factors $\nu = 1.1$ and $\nu = 0.9$. A more careful analysis shows that the collective insulators at the lowest temperatures develop in the range of filling factors $0.83 \lesssim \nu \lesssim 0.93$ and $1.06 \lesssim \nu \lesssim 1.21$. IQHWSs are known collective insulators forming in the above ranges of filling factors. Indeed, the above ranges of filling factors overlap extremely well with those of IQHWSs observed in microwave absorption [10] and in tunneling measurements [27], and they are reasonably close to those from compressibility

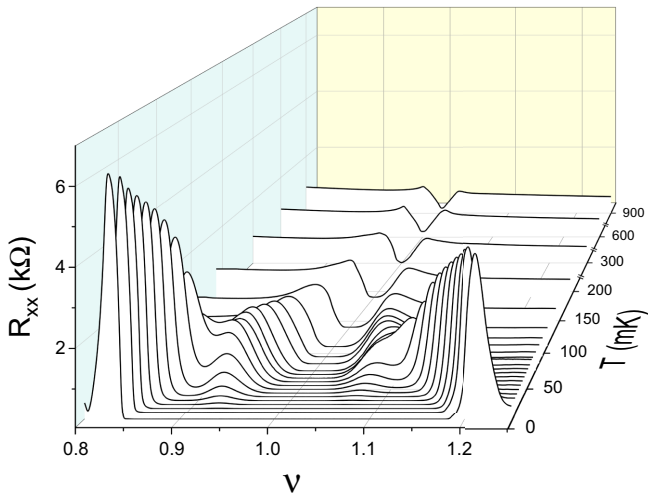

FIG. 2. The evolution of the longitudinal magnetoresistance R_{xx} at $\nu = 1$ in the ν-T parameter space for temperatures ranging from 10 to 900 mK. Line breaks were added between high-temperature traces.

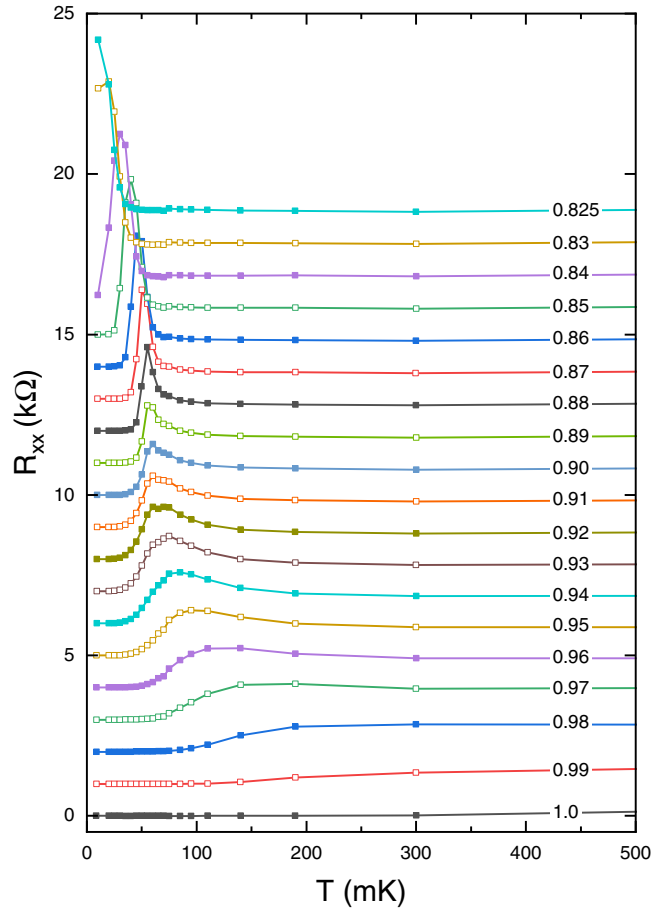

FIG. 3. Waterfall plot of $R_{xx}(T)|_{\nu=\text{fixed}}$ resistance profiles for $\nu = 1.0$ to 0.825. With the exception of the $\nu = 1$ trace, traces are vertically offset by 1 kΩ. The sharp resistance peaks that develop at $\nu \leqslant 0.90$ are associates with the IQHWS.

[24] and transport measurements [28]. Furthermore, according to Hartree-Fock calculations [5–8], single-electron BPs, i.e., Wigner solids, are the only collective insulators that may form in the lowest Landau levels at the above ranges of filling factors. Therefore, based on transport signatures, results of prior experiments [10,24,27,28], and based on consistency with theory, we interpret the collective ground states near the filling factors $\nu = 1.1$ and $\nu = 0.9$ as IQHWSs. Furthermore, we associate the part of the integer quantum Hall plateau between the two reentrant states with AI.

In the following, we analyze the temperature evolution of the magnetoresistance of the $\nu = 1$ integer quantum Hall plateau. We extract cuts along constant ν in the complex landscape of $R_{xx}(\nu, T)$, shown in Fig. 2. The resulting $R_{xx}(T)|_{\nu=\text{fixed}}$ resistance profiles obtained for various filling factors are shown in Fig. 3. Here we focus on the behavior of the $R_{xx}(T)|_{\nu=\text{fixed}}$ resistance profiles for $\nu \leqslant 1$; however, we note that a qualitatively similar trend is also observed for $\nu \geqslant 1$ (not shown in Fig. 3). For most traces in Fig. 3, $R_{xx} = 0$ at $T = 10$ mK, and thus the corresponding filling factors are associated with the plateau of the $\nu = 1$ IQHS. The most striking feature of the $R_{xx}(T)|_{\nu=\text{fixed}}$ resistance profiles is the sharp peak present at filling factors $\nu \leqslant 0.90$. At other filling factors, such as the ones in the $0.97 \leqslant \nu \leqslant 1$ range, the resistance profiles $R_{xx}(T)|_{\nu=\text{fixed}}$ display a gradual and monotonic decrease as T is lowered. Yet at other filling factors, such as at $\nu \approx 0.96$, in $R_{xx}(T)|_{\nu=\text{fixed}}$ there is a small and relatively broad local maximum; the peak resistance at $\nu \approx 0.96$ is barely above the flat background resistance value measured at higher temperatures. Since sharp peaks in the $R_{xx}(T)|_{\nu=\text{fixed}}$ resistance profile occur in the range of filling factors of the IQHWS, we surmise that they are a fundamental signature in the dc transport of this state.

Sharp peaks in $R_{xx}(T)|_{\nu=\text{fixed}}$ that resemble the ones shown in Fig. 3 for the IQHWS are also present for the BPs residing in the second and higher Landau levels [30–33], but are absent for the AI. We therefore suggest that a sharp peak in $R_{xx}(T)|_{\nu=\text{fixed}}$ is a shared property of all isotropic collective insulators forming in the flanks of integer quantum Hall plateaus, i.e., the IQHWSs and BPs at least in a restricted parameter space. We note that since the IQHWS is identical to the one-electron BP [5–8], it is reasonable that these phases, i.e., the multielectron and single-electron BPs, share similar transport properties. The temperature of the sharp peak in $R_{xx}(T)|_{\nu=\text{fixed}}$ can then be interpreted as the onset temperature T_{onset} of these collective insulators [30–33]. The largest onset temperature of IQHWS near $\nu = 0.90$ in our sample is $T_{\text{onset}} = 60$ mK, whereas near $\nu = 1.1$, $T_{\text{onset}} = 65$ mK.

To quantify the trends in the sharp resistive peaks in $R_{xx}(T)|_{\nu=\text{fixed}}$ and shown in Fig. 3, we define the peak sharpness parameter (PSP) as the ratio of the R_{xx} peak height relative to R_{xx} ($T = 190$ mK), a measure of the flat resistive background at high temperatures, and the width ΔT_{peak} at half height, as measured in mK. Such a parameter becomes large when the peak becomes prominent, i.e., when the peak height increases and when its width becomes narrow. The PSP is thus useful for quantifying the sharpening of resistance peaks seen in Fig. 3. PSP values extracted this way are plotted as a function of the filling factor in Fig. 4. In the $0.90 < \nu < 0.955$ range, the PSP changes little with ν. In this range of filling

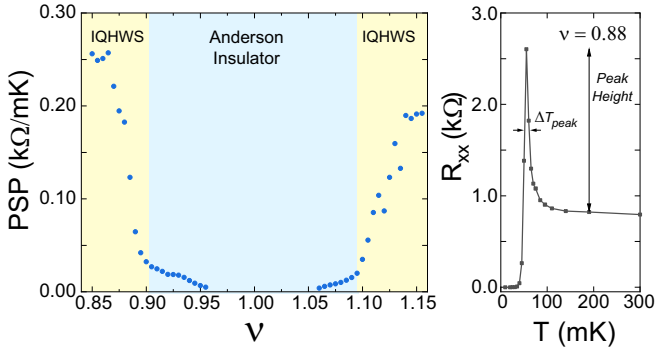

FIG. 4. Plot of the peak sharpness parameter (PSP) plotted as a function of filling factor (left). $R_{xx}(T)$ at $\nu = 0.88$ (right) provides reference for the quantities used in calculating the PSP.

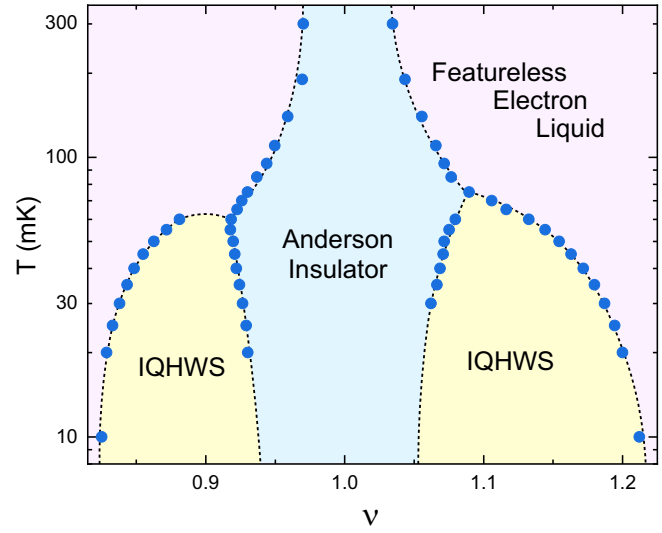

FIG. 5. Diagram in ν-T phase space of the localized AI and IQHWS phases near $\nu = 1$. Blue dots mark the filling factors of the local maxima of $R_{xx}(\nu)|_{T=\text{fixed}}$ curves. Dashed lines are guides to the eye.

factors, $R_{xx}(T)|_{\nu=\text{fixed}}$ profiles have the small, broad peak present. For $\nu < 0.90$, where the $R_{xx}(T)|_{\nu=\text{fixed}}$ profiles exhibit a sharp peak, there is a precipitous increase of the PSP. The sudden increase of the PSP at $\nu = 0.90$ thus signals the onset of the IQHWS. At larger filling factors, we find a similar onset of the IQHWS near $\nu = 1.095$. Each of these two filling factors can be thought of as the demarcation point between the IQHWS and the AI on the filling factor axis.

In our interpretation, at $T \ll T_{\text{onset}}$, the IQHWS is stable and is fully localized; at $T \gg T_{\text{onset}}$, the ground state is an electron liquid; and at $T \approx T_{\text{onset}}$, there is a network of interpenetrating domains of the IQHWS and electron liquid. The presence of the sharp resistive peak in the $R_{xx}(T)|_{\nu=\text{fixed}}$ profiles as T is scanned is a result of increased scattering along the domain walls of interpenetrating domains of these two phases. Similarly, the local maxima in $R_{xx}(B)|_{T=\text{fixed}}$, such as the ones labeled by $*$ symbols for the $T = 55$ mK shown in Fig. 1, can also be understood as originating from enhanced scattering. We notice that the height of the local resistance maxima in the $R_{xx}(B)|_{T=55\text{mK}}$ trace shown in Fig. 1 is larger when the IQHWS-to-electron liquid boundary is crossed at $B = 2.71$ T and at $B = 3.56$ T and is considerably less across the IQHWS-to-AI boundary at $B = 2.89$ T and at $B = 3.38$ T.

IV. THE INTEGER QUANTUM HALL PLATEAU IN THE ν-T PHASE SPACE

While the data shown in Fig. 3 highlight a sudden change as one crosses the AI-to-IQHWS boundary, it does not depict this boundary in the ν-T phase space. In order to obtain such a diagram, we use the local maxima of $R_{xx}(B)|_{T=\text{fixed}}$, such as the ones marked by $*$ symbols for the $R_{xx}(B)|_{T=55\text{mK}}$ shown in Fig. 1. We associate different localized phases to the different regions between the local maxima in such traces. As an example, the sequence of IQHWS, AI, and IQHWS in the trace of $R_{xx}(B)|_{T=55\text{mK}}$ shown in Fig. 1 is associated with the following range of magnetic fields: 2.71 to 2.89 T, 2.89 to 3.38 T, and 3.38 to 3.56 T, respectively. The blue dots in Fig. 5 represent the boundary of the localized states obtained this way in the ν-T phase space. The boundaries with the featureless electron liquid are a measure of the width of the plateau of the $\nu = 1$ IQHS. At the highest shown temperature, we have only the AI, which occupies an increasingly wider range of filling factors as the temperature is dropped. This boundary, however, bifurcates and the width of the integer quantum Hall plateau increases significantly as the temperature reaches values less than 65 mK, at which point the IQHWS sets in. These transport features thus allow us to define a boundary between the AI and the IQHWS. However, at the lowest temperature reached, transport no longer exhibits any features to distinguish the AI and IQHWS, and thus for tracing the phase boundary here, other techniques will have to be employed. Our suggested boundary between the two different localized states at these low temperatures is extrapolated from the boundary present at higher temperatures, and it is aided by the expectation that this boundary does not shift significantly.

V. DISCUSSION

The formation of collective insulators, such as the IQHWS, in the presence of disorder remains a challenging problem with many unanswered questions. We associated the reentrant integer quantum Hall effect forming near $\nu = 1.1$ and $\nu = 0.9$ with the IQHWS. However, the absence of reentrant behavior does not necessarily mean the absence of the IQHWS. Indeed, with the exception of Ref. [28], prior transport work on lower mobility samples near $\nu = 1.1$ and $\nu = 0.9$ did not exhibit reentrance, but the IQHWS was found to develop using techniques other than transport [10,24,26,27]. We thus suspect that reentrant transport features studied in this paper develop only in samples with very low levels of disorder and with the highest mobility. At this time, conditions under which IQHWSs exhibit reentrant transport and thus can be differentiated from the AI in transport measurements remain unclear. We propose that the morphology of the interpenetrating domains of the IQHWS and electron liquid, i.e., the domain size of the IQHWS in particular, may play a role.

We found that magnetoresistance patterns near $\nu = 2$ are different from those near $\nu = 1$. Indeed, as seen in Fig. 1, reentrance of the IQHS is absent in our sample near $\nu = 2$ down to the lowest temperatures studied. This is puzzling since IQHWSs were observed near $\nu = 2$ in microwave absorption [10], nuclear magnetic resonance [25], and surface acoustic wave measurements [26] in samples of lower mobility than ours. Other work on the IQHWS did not examine or report on data near $\nu = 2$ [27,28]. We do not have an explanation for the lack of reentrance of the IQHS near $\nu = 2$. One possibility is that the IQHWSs also form there, but in our sample, transport signatures associated with the IQHWS are not present. Such an explanation is consistent with early observation near $\nu = 1$, where microwave spectroscopy found signatures of IQHWSs, but early transport measurements did not find a reentrant behavior. In an earlier paragraph, we ascribed the presence of enhanced resistance associated with reentrance as being due to enhanced scattering of interpenetrating domains of an electron solid and liquid. We think that the lack of reentrance is likely influenced by the temperature-dependent length scales of these domains. Another possibility is that the IQHWS does not form near $\nu = 2$. The stability of Wigner solids is known to be affected not just by disorder, but also by sample parameters such as the width of the quantum well and Landau level mixing. One possibility is thus that in our sample, such effects destabilize the IQHWS near $\nu = 2$.

It is important to appreciate that the diagram shown in Fig. 5 will depend on the disorder. For example, the filling factor ranges for the IQHWS and the onset temperatures of the IQHWS will depend on disorder levels. While it is generally thought that disorder suppresses a collective phase such as the IQHWS, under special circumstances disorder may stabilize a Wigner solid in a region where the Wigner solid did not form in the absence of disorder. Such a scenario was realized in samples in which a short-range disorder was embedded into the channel during the molecular beam epitaxy growth [35,36] and in which a Wigner solid developed near $\nu \approx 0.6$. Complex disorder effects are also likely at play in the formation of other collective insulators, such as the BPs in high Landau levels [20,21]. In addition, there is ample theoretical [5–8,37] and experimental evidence [21,28,38–41] that the short-range part of the electron-electron interaction tuned by parameters such as the width of the confining quantum well will impact the formation of various collective insulators. For example, results of microwave absorption measurements on samples with significantly lower mobility than ours found structures in the flanks of the $\nu = 1$ integer plateau that were interpreted as two distinct electron solids [38,39]. We thus expect that such parameters will also impact the stability diagram of the IQHWS. Lastly, as the disorder is further reduced, new ordered phases may appear in the region of the AI. However, characterizing the extremely low level of disorder and its spatial distribution in these samples is not possible with current technologies.

As discussed earlier, the IQHWS and the AI at intermediate temperatures are separated by a local maximum in the $R_{xx}(B)|_{T=\text{fixed}}$ curves. These local maxima were used to identify the IQHWS and to draw the phase stability diagram shown in Fig. 5. However, at the lowest temperatures, we do not detect these local maxima. This situation is reminiscent of the transport behavior in high Landau levels, where in a large number of experiments a local maximum was reported separating multielectron BPs from the integer plateau [16–18] or separating different multielectron BPs [20,21]. However, there are known exceptions to this rule. In some samples or for some sample parameters, these local maxima between the BP and the integer plateau are either not present [42–45] or are present at intermediate temperatures but absent at the lowest temperatures [21,46–48]. This latter behavior is similar to the behavior of local maxima separating the IQHWS and the AI that we observe. Due to the lack of a detailed model for transport, we cannot offer an explanation for such a behavior. However, we suggest that since the enhanced scattering is due to interpenetrating domains of competing phases, it is likely that the temperature-dependent local resistance maximum is influenced by the temperature-driven change of the domain sizes.

Finally, we note that IQHWSs near $\nu = 1$ have spin texture [49–54]. Since our measurements are sensitive only to electron localization, we cannot access any information on magnetic ordering, pertaining, for example, to skyrmion formation.

In summary, we studied the complex structure of the magnetotransport near the $\nu = 1$ IQHS forming in the newest class of high-mobility 2DEGs. Transport in the flanks of the $\nu = 1$ exhibits reentrance and the region of reentrance was associated with the IQHWS. We found that the $R_{xx}(T)_{\nu=\text{fixed}}$ resistance profiles exhibit a sharp peak. Such sharp peaks in the $R_{xx}(T)_{\nu=\text{fixed}}$ resistance profiles were previously reported in the BPs, and thus these peaks appear to be present for all isotropic electron solids that form in low-disorder 2DEGs. The temperature of this sharp peak was assigned to the onset of the IQHWS. Finally, we also presented a phase stability diagram in ν-T space of the AI and the IQHWS near the $\nu = 1$ integer quantum Hall plateau.

ACKNOWLEDGMENTS

Measurements at Purdue University were supported by the NSF Grant No. DMR 1904497. Sample growth efforts of L.N.P. and K.W.W. were supported by the NSF MRSEC Grant No. DMR-1420541 and the Gordon and Betty Moore Foundation Grant No. GBMF 4420.

[1] R. B. Laughlin, Phys. Rev. B **23**, 5632 (1981).
[2] H. Aoki and T. Ando, Solid State Commun. **38**, 1079 (1981).
[3] B. I. Halperin, Phys. Rev. B **25**, 2185 (1982).
[4] K. von Klitzing, G. Dorda, and M. Pepper, Phys. Rev. Lett. **45**, 494 (1980).
[5] A. A. Koulakov, M. M. Fogler, and B. I. Shklovskii, Phys. Rev. Lett. **76**, 499 (1996).
[6] M. M. Fogler, A. A. Koulakov, and B. I. Shklovskii, Phys. Rev. B **54**, 1853 (1996).
[7] R. Moessner and J. T. Chalker, Phys. Rev. B **54**, 5006 (1996).

[8] M. M. Fogler and A. A. Koulakov, Phys. Rev. B **55**, 9326 (1997).

[9] F. D. M. Haldane, E. H. Rezayi, and K. Yang, Phys. Rev. Lett. **85**, 5396 (2000).

[10] Y. P. Chen, R. M. Lewis, L. W. Engel, D. C. Tsui, P. D. Ye, L. N. Pfeiffer, and K. W. West, Phys. Rev. Lett. **91**, 016801 (2003).

[11] R. M. Lewis, Y. Chen, L. W. Engel, D. C. Tsui, P. D. Ye, L. N. Pfeiffer, and K. W. West, Phys. Rev. Lett. **93**, 176808 (2004).

[12] R. M. Lewis, Yong P. Chen, L. W. Engel, D. C. Tsui, P. D. Ye, L. N. Pfeiffer, and K. W. West, Physica E (Amsterdam) **22**, 104 (2004).

[13] H. W. Jiang, R. L. Willett, H. L. Stormer, D. C. Tsui, L. N. Pfeiffer, and K. W. West, Phys. Rev. Lett. **65**, 633 (1990).

[14] V. J. Goldman, M. Santos, M. Shayegan, and J. E. Cunningham, Phys. Rev. Lett. **65**, 2189 (1990).

[15] H. A. Fertig and M. Shayegan, in *Perspectives in Quantum Hall Effects*, edited by S. Das Sarma and A. Pinczuk (Wiley, New York, 1997).

[16] M. P. Lilly, K. B. Cooper, J. P. Eisenstein, L. N. Pfeiffer, and K. W. West, Phys. Rev. Lett. **82**, 394 (1999).

[17] R. R. Du, D. C. Tsui, H. L. Stormer, L. N. Pfeiffer, K. W. Baldwin, and K. W. West, Solid State. Commun. **109**, 389 (1999).

[18] K. B. Cooper, M. P. Lilly, J. P. Eisenstein, L. N. Pfeiffer, and K. W. West, Phys. Rev. B **60**, R11285 (1999).

[19] J. P. Eisenstein, K. B. Cooper, L. N. Pfeiffer, and K. W. West, Phys. Rev. Lett. **88**, 076801 (2002).

[20] X. Fu, Q. Shi, M. A. Zudov, G. C. Gardner, J. D. Watson, and M. J. Manfra, Phys. Rev. B **99**, 161402(R) (2019).

[21] D. Ro, N. Deng, J. D. Watson, M. J. Manfra, L. N. Pfeiffer, K. W. West, and G. A. Csáthy, Phys. Rev. B **99**, 201111(R) (2019).

[22] S. Chen, R. Ribeiro-Palau, K. Yang, K. Watanabe, T. Taniguchi, J. Hone, M. O. Goerbig, and C. R. Dean, Phys. Rev. Lett. **122**, 026802 (2019).

[23] H. Zhou, H. Polshyn, T. Taniguchi, K. Watanabe, and A. F. Young, Nat. Phys. **16**, 154 (2020).

[24] D. Zhang, X. Huang, W. Dietsche, K. von Klitzing, and J. H. Smet, Phys. Rev. Lett. **113**, 076804 (2014).

[25] L. Tiemann, T. D. Rhone, N. Shibata, and K. Muraki, Nat. Phys. **10**, 648 (2014).

[26] I. L. Drichko, I. Yu. Smirnov, A. V. Suslov, L. N. Pfeiffer, K. W. West, and Y. M. Galperin, Phys. Rev. B **92**, 205313 (2015).

[27] J. Jang, B. M. Hunt, L. N. Pfeiffer, K. W. West, and R. C. Ashoori, Nat. Phys. **13**, 340 (2017).

[28] Y. Liu, C. G. Pappas, M. Shayegan, L. N. Pfeiffer, K. W. West, and K. W. Baldwin, Phys. Rev. Lett. **109**, 036801 (2012).

[29] Y. J. Chung, K. A. Villegas Rosales, K. W. Baldwin, P. T. Madathil, K. W. West, M. Shayegan, and L. N. Pfeiffer, Nat. Mater. **20**, 632 (2021).

[30] N. Deng, A. Kumar, M. J. Manfra, L. N. Pfeiffer, K. W. West, and G. A. Csáthy, Phys. Rev. Lett. **108**, 086803 (2012).

[31] N. Deng, J. D. Watson, L. P. Rokhinson, M. J. Manfra, and G. A. Csáthy, Phys. Rev. B **86**, 201301(R) (2012).

[32] W. E. Chickering, Ph.D. thesis, California Institute of Technology, 2015.

[33] D. Ro, S. A. Myers, N. Deng, J. D. Watson, M. J. Manfra, L. N. Pfeiffer, K. W. West, and G. A. Csáthy, Phys. Rev. B **102**, 115303 (2020).

[34] N. Samkharadze, A. Kumar, M. J. Manfra, L. N. Pfeiffer, K. W. West, and G. A. Csáthy, Rev. Sci. Instrum. **82**, 053902 (2011).

[35] W. Li, D. R. Luhman, D. C. Tsui, L. N. Pfeiffer, and K. W. West, Phys. Rev. Lett. **105**, 076803 (2010).

[36] B.-H. Moon, L. W. Engel, D. C. Tsui, L. N. Pfeiffer, and K. W. West, Phys. Rev. B **92**, 035121 (2015).

[37] R. Price, X. Zhu, S. Das Sarma, and P. M. Platzman, Phys. Rev. B **51**, 2017 (1995).

[38] A. T. Hatke, Y. Liu, B. A. Magill, B. H. Moon, L. W. Engel, M. Shayegan, L. N. Pfeiffer, K. W. West, and K. W. Baldwin, Nat. Commun. **5**, 4154 (2014).

[39] A. T. Hatke, Y. Liu, L. W. Engel, L. N. Pfeiffer, K. W. West, K. W. Baldwin, and M. Shayegan, Phys. Rev. B **98**, 195309 (2018).

[40] K. A. Schreiber, N. Samkharadze, G. C. Gardner, Y. Lyanda-Geller, M. J. Manfra, L. N. Pfeiffer, K. W. West, and G. A. Csáthy, Nat. Commun. **9**, 2400 (2018).

[41] K. A. Schreiber and G. A. Csáthy, Annu. Rev. Condens. Matter Phys. **11**, 17 (2020).

[42] K. B. Cooper, M. P. Lilly, J. P. Eisenstein, L. N. Pfeiffer, and K. W. West, Phys. Rev. B **65**, 241313(R) (2002).

[43] Y. Liu, D. Kamburov, M. Shayegan, L. N. Pfeiffer, K. W. West, and K. W. Baldwin, Phys. Rev. B **87**, 075314 (2013).

[44] G. Gamez and K. Muraki, Phys. Rev. B **88**, 075308 (2013).

[45] B. Friess, Y. Peng, B. Rosenow, F. von Oppen, V. Umansky, K. von Klitzing, and J. H. Smet, Nat. Phys. **13**, 1124 (2017).

[46] J. P. Eisenstein, M. P. Lilly, K. B. Cooper, L. N. Pfeiffer, and K. W. West, Physica E **6**, 29 (2000).

[47] X. Wang, H. Fu, L. Du, X. Liu, P. Wang, L. N. Pfeiffer, K. W. West, R. R. Du, and X. Lin, Phys. Rev. B **91**, 115301 (2015).

[48] K. Bennaceur, C. Lupien, B. Reulet, G. Gervais, L. N. Pfeiffer, and K. W. West, Phys. Rev. Lett. **120**, 136801 (2018).

[49] S. E. Barrett, G. Dabbagh, L. N. Pfeiffer, K. W. West, and R. Tycko, Phys. Rev. Lett. **74**, 5112 (1995).

[50] V. Bayot, E. Grivei, S. Melinte, M. B. Santos, and M. Shayegan, Phys. Rev. Lett. **76**, 4584 (1996).

[51] W. Desrat, D. K. Maude, M. Potemski, J. C. Portal, Z. R. Wasilewski, and G. Hill, Phys. Rev. Lett. **88**, 256807 (2002).

[52] G. Gervais, H. L. Stormer, D. C. Tsui, P. L. Kuhns, W. G. Moulton, A. P. Reyes, L. N. Pfeiffer, K. W. Baldwin, and K. W. West, Phys. Rev. Lett. **94**, 196803 (2005).

[53] H. Zhu, G. Sambandamurthy, Y. P. Chen, P. Jiang, L. W. Engel, D. C. Tsui, L. N. Pfeiffer, and K. W. West, Phys. Rev. Lett. **104**, 226801 (2010).

[54] W. Desrat, B. A. Piot, S. Krämer, D. K. Maude, Z. R. Wasilewski, M. Henini, and R. Airey, Phys. Rev. B **88**, 241306(R) (2013).